Real-time PEGDA-based microgel generation and encapsulation in microdroplets

Martino, Chiara; Vigolo, Daniele; Solvas, Xavier Casadevall i; Stavrakis, Stavros; deMello, Andrew J.

DOI:
10.1002/admt.201600028

Real-time PEGDA-based Microgel Generation and Encapsulation in Microdroplets

Chiara Martino[1*+], Daniele Vigolo[2*+], Xavier Casadevall i Solvas[1], Stavros Stavrakis[1], Andrew J. deMello[1*]

[1] Institute for Chemical and Bioengineering, Department of Chemistry and Applied Biosciences, ETH Zurich, Vladimir Prelog Weg 1, Zürich 8093, Switzerland; [2] School of Chemical Engineering, University of Birmingham, Edgbaston, Birmingham, B15 2TT, UK; [+] Equal contribution.

[*] Correspondence: c.martino@tue.nl, daniele.vigolo@chem.ethz.ch, andrew.demello@chem.ethz.ch,

Herein we report a method that combines droplet-based microfluidics and microscope projection photolithography for the generation of PEGDA microgels and their encapsulation within pL-volume droplets. By implementing continuous-flow photolithography in the vicinity of a cross junction, we demonstrate the real-time generation and *in situ* encapsulation of fiber-like structures within pL-volume aqueous microdroplets. We assess the effect of UV excitation at varying distances from the cross junction for both constant and pulsed UV excitation modes, as a route to controlling microfiber length. Finally, we explore UV excitation within trapped droplets and demonstrate how the combination of the two techniques can lead to the generation of 3D patterned micro-structures, opening new avenues for the rapid generation of inner scaffolding of artificial cell facsimiles.

1 Introduction

Microgels are cross-linked polymer networks that are employed in a broad range of biomedical applications(1). Specifically, microgels are commonly used as biomaterials for the construction of scaffolds in tissue engineering(2, 3) and drug delivery applications(4, 5), sensors in diagnostics(6, 7) and artificial cells in therapeutic applications(8).

Recent advances in microgel synthesis have contributed towards an improved control over their chemical, physical, mechanical and morphological characteristics(9). In this regard, microfluidics has shown enormous potential in not only providing robust methods for the production of monodisperse geometries but also in increasing, space-time yields and the range of microgel morphologies(1, 9).

Of particular relevance in regard to the production of precisely shaped polymeric particles is continuous flow photolithography(10), which uses projection photolithography to form polymerized hydrogels within flow based environments. Doyle *et al.*(10) elegantly demonstrated that UV illumination of a flowing precursor solution containing poly ethylene glycol diacrylate (PEGDA) and a photoinitiator within a microchannel can controllably and rapidly produce micron-sized polymeric structures through elongation of the UV pattern. Furthermore, the same authors also demonstrated that through synchronization and interruption of the flow, it is possible to synthesize polymeric structures with extremely high resolution and feature sizes down to colloidal length scales(11). This technique, commonly called stop-flow lithography, has been successfully used for the generation of cell-laden hydrogels(12), shape-evolving degradable microgels(13) and superparamagnetic particles(14).

Inspired by the above studies, we herein combine continuous flow lithography with droplet-based microfluidics to explore the effects of UV excitation of a precursor PEGDA solution in the vicinity of a cross junction. Based on these investigations, we also demonstrate the application of microscope projection photolithography in trapped droplets for the first time. It has been previously shown that in the radical-induced polymerization of PEGDA, cross-linking of free radicals is inhibited when molecular oxygen binds to a photoinitiator molecule(15). Herein we take advantage of the gas permeability of polydimethylsiloxane (PDMS) to perform PEGDA polymerization in two different formats: "*in*" and "*all-in*" PDMS, which differ only through the presence or lack of a bottom PDMS layer in the microfluidic reactor (Figure 1). The *all-in* PDMS device not only prevents PEGDA from crosslinking onto the bottom glass slide but also allows polymerized PEGDA species to remain suspended within the microchannel (Figure 1a). By definition, crosslinking of PEGDA onto the glass substrate is also avoided within confined droplets dispersed in an oil phase (Figure 1b). We utilize both formats and demonstrate how different photo-patterning geometries, depicted in Figure 1c-e, can be used to generate microgel structures of controlled geometries, which, we suggest, can find a variety of uses in the generation of scaffolds in cell-based assays(16) and artificial cell constructs(17-19). Finally, we also investigate the synergistic effect of droplet-based microfluidics and continuous flow lithography by adopting the ghost particle velocimetry (GPV) analysis(20), to rapidly probe the flow field(20, 21).

2 Experimental

Materials

Microdroplets were generated using a continuous phase of fluorinated oil (FC40, 3M, USA) containing 4% PFPE–PEG–PFPE surfactant (synthesized in house). The dispersed phase was made from a solution containing 54% (v/v) poly(ethylene glycol) (MW 575) diacrylate (PEGDA, Sigma,

Switzerland), 44% (v/v) deionized water and 2% or 4% (v/v) UV curing agent (Darocur 1173, Ciba, Switzerland). For the GPV analysis, the dispersed phase consisted of a solution containing 54% (v/v) PEGDA, 42% (v/v) of DI water, 2% (v/v) of UV curing agent and 2% (v/v) of polystyrene beads solution (0.2% v/v, 0.20 µm, F8809, Life Technologies, Switzerland). Both solutions were regulated using a pressure controller (OB1, Elveflow, France).

Experimental setup

All microfluidic device designs included channels for the introduction of dispersed and continuous phases and a cross junction for droplet generation. The droplet trapping device comprised either a single trap or a series of traps immediately after the droplet generation point (designs provided in the ESI). Microfluidic devices were fabricated using standard softlithography methods(22) in Polydimethylsiloxane (PDMS, Sylgard 184, Dow Corning, USA) and with the PDMS base and curing agent mixed at a ratio of 10:1. The height of the channels and the diameter of the orifice at the cross junction were 48 and 75 µm respectively. PDMS molds were irreversibly bonded to 130-160 µm thick glass coverslips (24 mm x 60 mm, Menzer Glaser, USA) coated with a 50 µm layer of PDMS (obtained by spin-coating the glass slides at 3000 rpm for 30 s). The devices used for droplet trapping were directly bonded onto uncoated glass slides.

All optical measurements were performed using an inverted microscope (Ti-E, Nikon, Switzerland) equipped with a 20X objective (NA 0.45, Nikon, Switzerland) and a 40X objective (NA 0.65, Nikon, Switzerland), a mercury lamp (100 W, Intensilight, Nikon, Switzerland) as an ultraviolet light source and an excitation bandpass filter (377/50 BrightLine HC, AHF, Germany). A high speed filter wheel system (HF110A, Prior Scientific, UK) was used as a shutter to provide either constant or intermittent UV illumination, with an ON/OFF switching speed of less than 50 ms. Two different CMOS cameras were used for video recordings: a high resolution and high sensitivity

camera (Hamamatsu ORCA-Flash4.0, Japan) and a high speed camera (Phantom Miro M310, Vision Research, USA) used exclusively for the GPV analysis. The synchronization of illumination and image acquisition was controlled by Micro-manager control software(23). To achieve PEGDA polymerization, a high-resolution transparency photomask was placed at the field stop plane of the microscope along the UV illumination path containing the desired pattern. Accordingly, a distribution profile of the light intensity based on the pattern is then projected into the PDMS microchannel through the objective. Photomasks were designed in AUTOCAD 2014 (Autodesk, USA) and printed using a high-resolution printer (Micro Lithography Services Ltd, UK). Videos were analyzed using ImageJ 1.48v software (NIH, Bethesda, USA).

3 Results and Discussion

Constant and pulsed UV excitation during PEGDA droplet formation

For continuous flow lithography, UV light was maintained at 100 W allowing the mask pattern to be continuously projected inside the channel, at set distances from the droplet-generating cross junction. Under these conditions PEGDA could be polymerized into a fiber, which was subsequently encapsulated inside a forming droplet. This process required fine control over the pressure of the two phases to ensure both a gradual flow of the dispersed phase and constant synchronized droplet generation. Typically both phases were delivered at 60 mbar, and as soon as UV illumination commenced photopolymerization initiated, with a fiber forming and elongating until it detaches and is then encapsulated into a droplet (**Figure 2a-f** and **Video 1** in the ESI). The full cycle of fiber formation and encapsulation can be defined using three characteristic time periods denoted as: *delay* (t_d), *formation* (t_f) and *encapsulation* (t_e). The first (t_d) begins when the first droplet pinches off and ends when PEGDA begins to polymerize (**Figure 2a-b**). During the formation phase (t_f), the PEGDA fiber becomes visible and elongates until the moment of

detachment (**Figure 2c**). The encapsulation phase (t_e) begins with the detachment of the fiber, proceeds with its incorporation into the forming droplet and ends with droplet pinch-off (**Figure 2d-e**).

We observe that the position at which UV illumination occurs clearly affects the fiber length (L_f). For instance, an increase in the distance between the excitation point and the cross junction (d_{je}) leads to the generation of longer fibers and a change in the frequency of droplet formation (**Figure 2g**). In addition, the duration of t_d, t_f *and* t_e are all affected by d_{je}, as shown in **Figure 2h**; for example for d_{je}>150 μm, the encapsulation time can be more than twice that when operating at smaller d_{je}. At higher d_{je} fiber encapsulation and droplet generation become desynchronized.

Intuitively the fiber length is primarily affected by two parameters: the spot size of UV light produced by the microscope objective and the local velocity of the fluid at that point. Together, these two parameters largely determine the exposure time. This means that if the flow rate is faster than the minimum exposure time necessary to polymerize the PEGDA, no polymerization will occur. As discussed later, our GPV analysis suggests that the event of droplet generation has a decisive effect both on fiber generation and termination.

Keeping the previous operational conditions constant (both phases at 60 mbar, and 100W illumination), the excitation point was then translated past the droplet-generating cross junction, so that the illumination focus was located within the "forming droplet" region. As shown in **Figure 3a** and **Video 2** the PEGDA polymerization process closely follows the streamlines inside the droplet, yielding curved fibers. When a second excitation spot is added (through modification of the photomask) as presented in **Figure 3b**, the droplet generation frequency decreases to approximately 0.59 s^{-1} (from the 0.39 s^{-1} for a single excitation spot). We believe that this is due to a local increase in viscosity induced by the UV illumination.

Within the "forming droplet" region, and at the same operational conditions, a single dot (**Figure 1c**) pulsed excitation was performed at a duty cycle (*D*) of 40% and a period equal to 0.5 s (meaning that illumination was "ON" for 0.2 s and then "OFF" for 0.3 s). Under these conditions we found that 0.2 s was the minimum time for which PEGDA crosslinking could be observed and three small fibers were formed and immediately encapsulated into the forming droplet (**Figure 4a**). Maintaining the same excitation cycle, the illumination point was focused 140 μm upstream of the droplet-forming cross junction (**Figure 4b**). This simple modification induced a slight increase in fiber length (**Figure 4c**) but did not change the number of fibers produced or the droplet generation frequency, whose value was comparable to that for continuous excitation at the same position (**Figure 4g**). Similarly, we performed pulsed illumination 215 μm upstream of the cross junction and studied the effects of different pulsation conditions on the length of the fibers. **Figure 4d** reports the fiber lengths obtained under each excitation condition, represented on the x-axis as $t_{ON}\_t_{OFF}$, namely the periods that the UV illumination was kept ON (t_{ON}) and OFF (t_{OFF}). As in previous cases, pulsed illumination affects only the fiber length with no significant alteration in the droplet generation frequency being observed.

Ghost Particle Velocimetry analysis of fiber generation

Ghost Particle Velocimetry (GPV) was used to quantify the effect of flow rate (during droplet production) on the PEGDA fiber at different d_{je}. As noted previously, the dispersed phase was seeded with 0.2 μm polystyrene particles at a concentration of 0.2 % v/v. When illuminated with white light via a condenser lens, light scattered by the nanoparticles generates a speckle pattern that is made visible by subtracting the median (obtained from multiple control images) from each frame recorded (**Figure 5a**)[16]. The speckle pattern is then analysed using standard Particle Image Velocimetry methods, i.e. each image is divided in small regions of interest and by performing

cross correlation analyses displacements calculated. Knowledge of the image acquisition frame rate allows extraction of the complete velocity field. ImageJ was used to analyse and manipulate images, and PIVlab(24) to perform velocimetry analysis. In particular, for each d_{je} tested, a 55 x 55 μm^2 region immediately behind the illumination spot was analysed (**Figure 5a-c**) to extract the average horizontal velocity *u*. Subsequently, the evolution of velocity with time was plotted (**Figure 5b**).

For each d_{je} (detailed in the ESI), we found a common oscillatory behaviour whose frequency was related to the droplet generation conditions. Typically, the velocity increased rapidly prior to droplet pinch-off and decreased after detachment of the droplet. By monitoring this process, we were able to determine a range of velocities over which the generation of fibers is possible. **Figure 5b** highlights this by reporting fiber formation at a d_{je} of 123 μm superposed with the flow velocity evolution. It is noticeable that fiber generation occurs when the average horizontal velocity is approximately 120 μm/s. This represents the velocity limit for which fibers can be generated. Fiber generation begins when the velocity of the flow is slower than the minimum exposure time required to polymerize the PEGDA solution, and continues until the flow rate is faster than this. The velocity limit is accordingly somewhere between these two values. As shown in the ESI this method provides consistent results over the range of d_{je} considered. Manipulation of the flow rate or the UV illumination exposure time, provides for control over the length of the fibers produced. Upon calibration this method can further be used to reliably produce (at high throughput), droplets containing a defined amount of fibers of a chosen geometry.

Constant and pulsed UV excitation in trapped droplets

We also investigated the effect of UV light excitation within trapped droplets containing a precursor PEGDA solution (under both moving and stationary conditions). For these experiments, the

concentration of the photoinitiator was 4% v/v. Initially, we used a pillar-based trap (**Figure 6**) for short-term trapping of continuously generated PEGDA droplets(25). As soon as a PEGDA droplet flows into such a trap, it displaces the previously trapped drop and remains there until the next droplet arrives and takes its place. Under constant UV light illumination, a single dot pattern (**Figure 1c**) was projected into the droplet and PEGDA crosslinking was observed. It was noted that crosslinking takes place only when the droplet is trapped for a sufficiently long period, as shown in the time sequence in **Figure 6 a-g**, and **Video 3** in the ESI. The trapping time of the droplet is directly related to the flow rate (or pressure drop) and the concentration of droplet in the continuous phase (i.e. the spacing between droplets). Once a trap is occupied, the droplet remains trapped until the following droplet reaches the same trap. For sufficiently spaced droplets and low flow rates it is possible to achieve a retention time of several seconds. In the example shown in Figure 6 the trapping time is equal to 5.1 s. After the emulsion is broken, curved microgels (such as those shown in **Figure 6h**) are clearly observed.

Experiments under stationary conditions were carried out using a different microfluidic device that allowed the generation and trapping of trains of PEGDA droplets in a linear array of traps (**Figure 7**). Here, as soon as the flow is interrupted droplets remain stationary (with no inner recirculation). Once stationary, UV excitation through a 0.65x NA objective was initiated using the patterning geometry shown in **Figure 1e**. UV excitation did not affect the droplet stability and microgels that perfectly matched the shape of the photomask patterns were generated inside the trapped droplets. **Figure 7** and **Video 4** in the ESI show trapped PEGDA droplets exposed to a 600 ms pulse of UV light passing through a photomask consisting of a row of repetitive dumbbell hexagons. Shorter UV pulses of 400 ms produced incomplete geometries as shown in **Video 5** in the ESI.

Conclusions

Herein we have demonstrated for the first time the combination of droplet-based microfluidics and continuous flow lithography. We show that such a combination allows the generation of PEGDA-based microgels of controlled geometry that are readily encapsulated into pL-volume droplets. Furthermore, we demonstrate that the dynamics of droplet generation are responsible for the self-regulation of the PEGDA fiber length produced by UV crosslinking. By simply manipulating the position of UV illumination and the length and the number of light pulses we are able to tune the number and the length of the produced microgels. Flow field mapping using Ghost Particle Velocimetry was successful in confirming that the oscillating flow dynamics induced by droplet generation are primarily responsible for the final length of the microgel fibers under constant UV illumination. In such oscillatory flows polymerization, and thus fiber generation, occurs only when the flow velocity is below a threshold determined by the photo-curing properties of the sample. Additionally, we have investigated the effects of UV excitation on trapped droplets under both static and dynamic conditions and proved that complex microgels geometries can be generated in a reproducible and high-throughput fashion. Finally, we believe that the method presented herein has great potential for the easy production of biocompatible microgels of controlled geometries, with potential future applications as scaffolds for artificial bio-inspired systems and cell-based studies being most obvious.

Acknowledgements

Chiara Martino and Daniele Vigolo acknowledge support from the ETH Zurich Postdoctoral Fellowship Program and Marie Curie Actions for People COFUND Program.

References

1. Tumarkin E, Kumacheva E. Microfluidic generation of microgels from synthetic and natural polymers. Chemical Society Reviews. 2009;38(8):2161-8.

2. Chung BG, Lee K-H, Khademhosseini A, Lee S-H. Microfluidic fabrication of microengineered hydrogels and their application in tissue engineering. Lab on a Chip. 2012;12(1):45-59.
3. Li C, Chen P, Shao Y, Zhou X, Wu Y, Yang Z, et al. A Writable Polypeptide–DNA Hydrogel with Rationally Designed Multi-modification Sites. Small. 2015;11(9-10):1138-43.
4. Langer R, Tirrell DA. Designing materials for biology and medicine. Nature. 2004;428(6982):487-92.
5. Kim S-H, Kim JW, Kim D-H, Han S-H, Weitz DA. Polymersomes Containing a Hydrogel Network for High Stability and Controlled Release. Small. 2013;9(1):124-31.
6. Islam MR, Ahiabu A, Li X, Serpe MJ. Poly (N-isopropylacrylamide) Microgel-Based Optical Devices for Sensing and Biosensing. Sensors (Basel, Switzerland). 2014;14(5):8984-95.
7. Rakickas T, Ericsson EM, Ruželė Ž, Liedberg B, Valiokas R. Functional Hydrogel Density Patterns Fabricated by Dip-Pen Nanolithography and Photografting. Small. 2011;7(15):2153-7.
8. Chang TMS. Therapeutic applications of polymeric artificial cells. Nat Rev Drug Discov. 2005;4(3):221-35.
9. Pelton R, Hoare T. Microgels and Their Synthesis: An Introduction. Microgel Suspensions: Wiley-VCH Verlag GmbH & Co. KGaA; 2011. p. 1-32.
10. Dendukuri D, Pregibon DC, Collins J, Hatton TA, Doyle PS. Continuous-flow lithography for high-throughput microparticle synthesis. Nat Mater. 2006;5(5):365-9.
11. Dendukuri D, Gu SS, Pregibon DC, Hatton TA, Doyle PS. Stop-flow lithography in a microfluidic device. Lab on a Chip. 2007;7(7):818-28.
12. Panda P, Ali S, Lo E, Chung BG, Hatton TA, Khademhosseini A, et al. Stop-flow lithography to generate cell-laden microgel particles. Lab on a Chip. 2008;8(7):1056-61.
13. Hwang DK, Oakey J, Toner M, Arthur JA, Anseth KS, Lee S, et al. Stop-Flow Lithography for the Production of Shape-Evolving Degradable Microgel Particles. Journal of the American Chemical Society. 2009;131(12):4499-504.
14. Suh SK, Yuet K, Hwang DK, Bong KW, Doyle PS, Hatton TA. Synthesis of Nonspherical Superparamagnetic Particles: In Situ Coprecipitation of Magnetic Nanoparticles in Microgels Prepared by Stop-Flow Lithography. Journal of the American Chemical Society. 2012;134(17):7337-43.
15. Decker C, Jenkins AD. Kinetic approach of oxygen inhibition in ultraviolet- and laser-induced polymerizations. Macromolecules. 1985;18(6):1241-4.
16. Tsuda Y, Morimoto Y, Takeuchi S. Monodisperse Cell-Encapsulating Peptide Microgel Beads for 3D Cell Culture. Langmuir. 2010;26(4):2645-9.
17. Martino C, Lee TY, Kim S-H, deMello AJ. Microfluidic generation of PEG-b-PLA polymersomes containing alginate-based core hydrogel. Biomicrofluidics. 2015;9(2):024101.
18. Martino C, Kim S-H, Horsfall L, Abbaspourrad A, Rosser SJ, Cooper J, et al. Protein Expression, Aggregation, and Triggered Release from Polymersomes as Artificial Cell-like Structures. Angewandte Chemie International Edition. 2012;51(26):6416-20.
19. Martino C, Statzer C, Vigolo D, deMello A. Controllable Generation and Encapsulation of Alginate Fibers Using Droplet-Based Microfluidics. Lab on a Chip. 2015.
20. Pirbodaghi T, Vigolo D, Akbari S, deMello A. Investigating the fluid dynamics of rapid processes within microfluidic devices using bright-field microscopy. Lab on a Chip. 2015;15(9):2140-4.
21. Buzzaccaro S, Secchi E, Piazza R. Ghost Particle Velocimetry: Accurate 3D Flow Visualization Using Standard Lab Equipment. Physical Review Letters. 2013;111(4):048101.
22. Xia YN, Whitesides GM. Soft lithography. Angewandte Chemie-International Edition. 1998;37(5):550-75.
23. Edelstein A, Amodaj N, Hoover K, Vale R, Stuurman N. Computer Control of Microscopes Using μManager. Current Protocols in Molecular Biology: John Wiley & Sons, Inc.; 2001.
24. Thielicke W, Stamhuis EJ. PIVlab - Time-Resolved Digital Particle Image Velocimetry Tool for MATLAB 2014/07/03.

25. Niu X, Gulati S, Edel JB, deMello AJ. Pillar-induced droplet merging in microfluidic circuits. Lab on a Chip. 2008;8(11):1837-41.

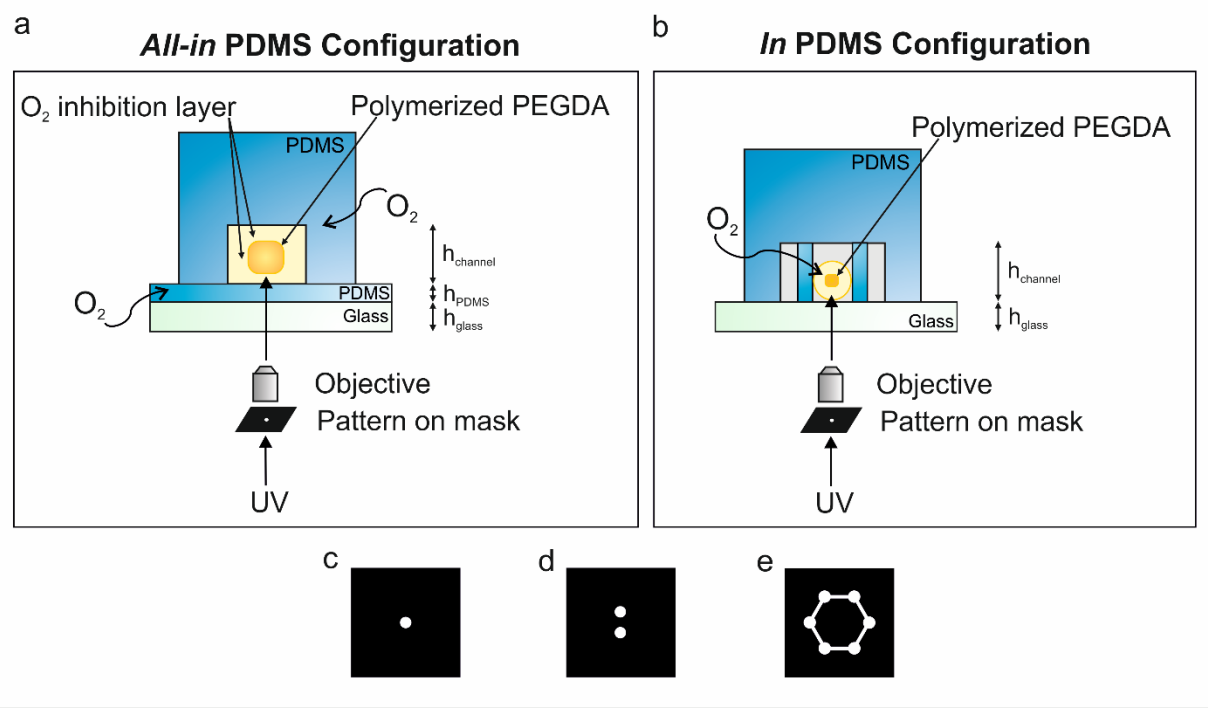

Figure 1. Combination of in-flow photolithography and droplet-based microfluidics. (a) Schematic view of the experimental setup used to achieve *in situ* polymerization of PEGDA within an "*all-in"* PDMS microchannel. The UV light passes through a high-resolution photomask with a desired pattern placed in the conjugated plane of the microscope. The pattern geometry is projected inside the microchannel where an aqueous PEGDA precursor phase flows. Since PEGDA polymerization is inhibited by oxygen and PDMS is oxygen permeable, PEGDA polymerization occurs in the innermost portion of the channel allowing the un-polymerised PEGDA to flow and carry the polymerised part away. In our experiments $h_{channel}$, h_{PDMS} and h_{glass} are equal to 45 µm, 50 µm and 130-160 µm respectively. (b) Schematic view of the experimental *"in"* PDMS configuration used for in-droplet PEGDA polymerization. The droplet containing un-crosslinked PEGDA is kept in position by traps composed of arrays of pillars where UV excitation can be performed. Since the un-polymerised PEGDA droplet is completely surrounded by an oil phase no

PDMS is required at the bottom of the device to prevent PEGDA build-up on that surface (which could lead to a blockage of the channel). (c-e) Geometries used for the generation of patterned PEGDA: (c) circle with diameter of 225 µm, (d) two circles with diameters of 225 µm and a centre-to-centre distance of 600 µm, (e) hexagon dumbbell pattern with a diameter of the circle equal to 100 µm and width of the arm equal to 25 µm.

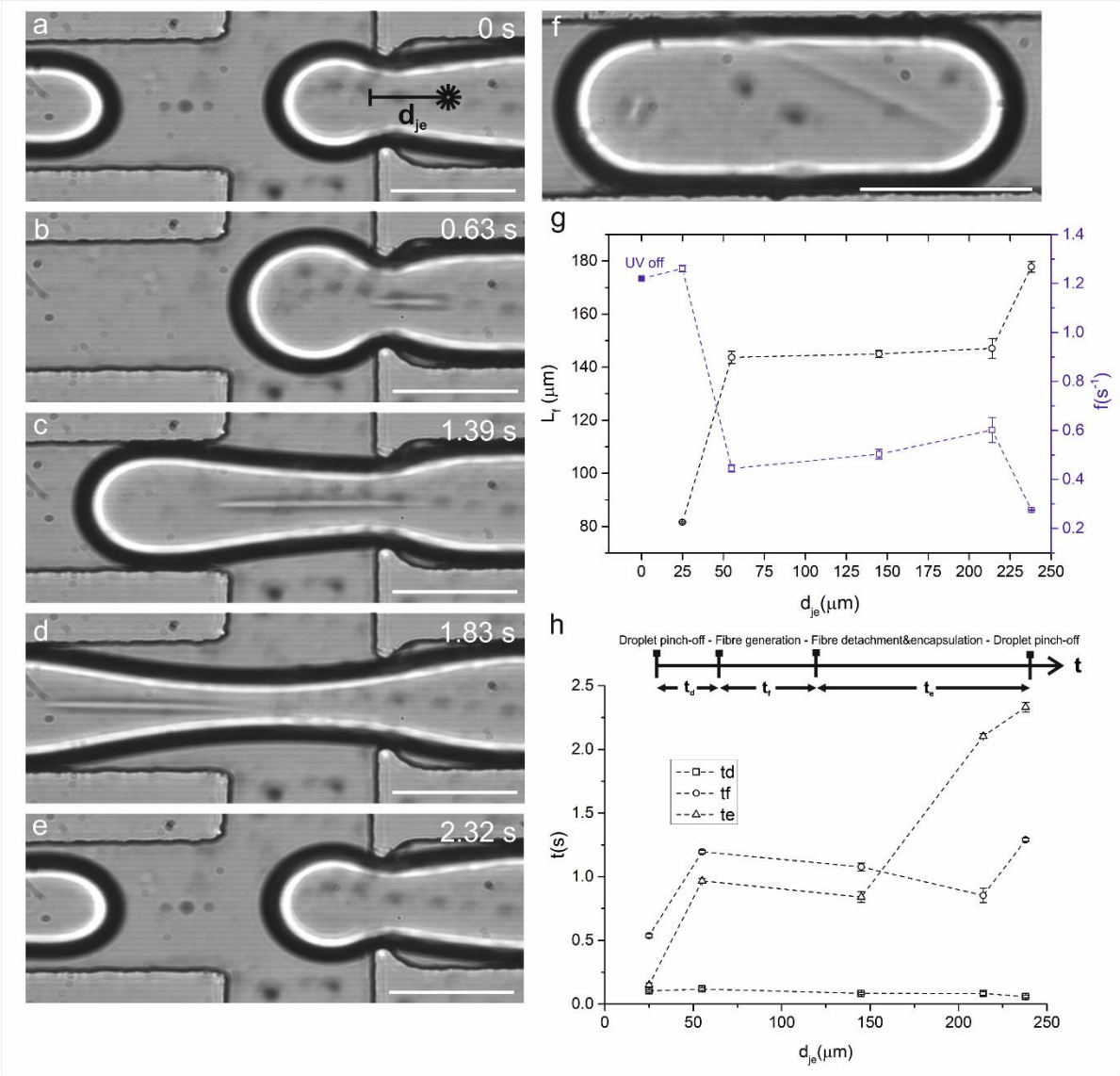

Figure 2. PEGDA fiber generation in a two-phase system and encapsulation into micro droplets. (a-f) Dispersed and continuous phase are both pressurized at 60 mbar and UV excitation occurs at 55 µm before the cross junction (d_{je}). In these conditions, fibers with an average length of 146 µm are generated and encapsulated into micro droplets, produced at a frequency of 0.44 s^{-1}. On average, at this distance, it takes 0.1 s for the polymerization to be initiated, 1.19 s for the fiber to be

generated and 0.96 s to be encapsulated. These times are also defined as t_d, t_f and t_e respectively. (g) Trend of fiber length and droplet generation frequency at different d_{je}. (h) Typical times of fiber formation and encapsulation in micro droplets. Scale bars are equal to 100 µm.

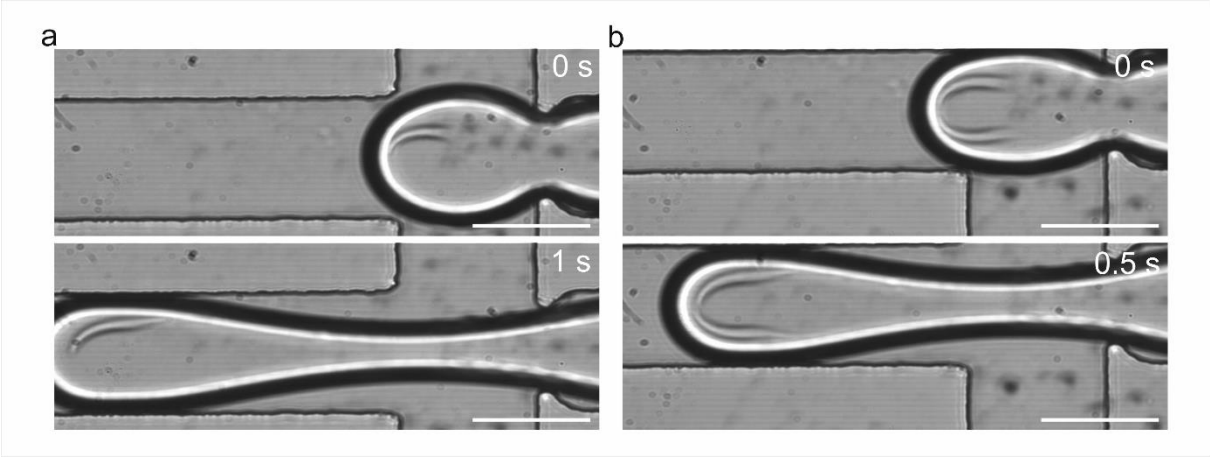

Figure 3. Constant UV excitation in droplets. Time lapse of (a) single dot and (b) double dot UV excitation pattern within the micro droplet during its formation. Both excitation conditions produced curved fibers due to the recirculation of fluid streamlines within the droplet. Scale bars are equal to 100 µm.

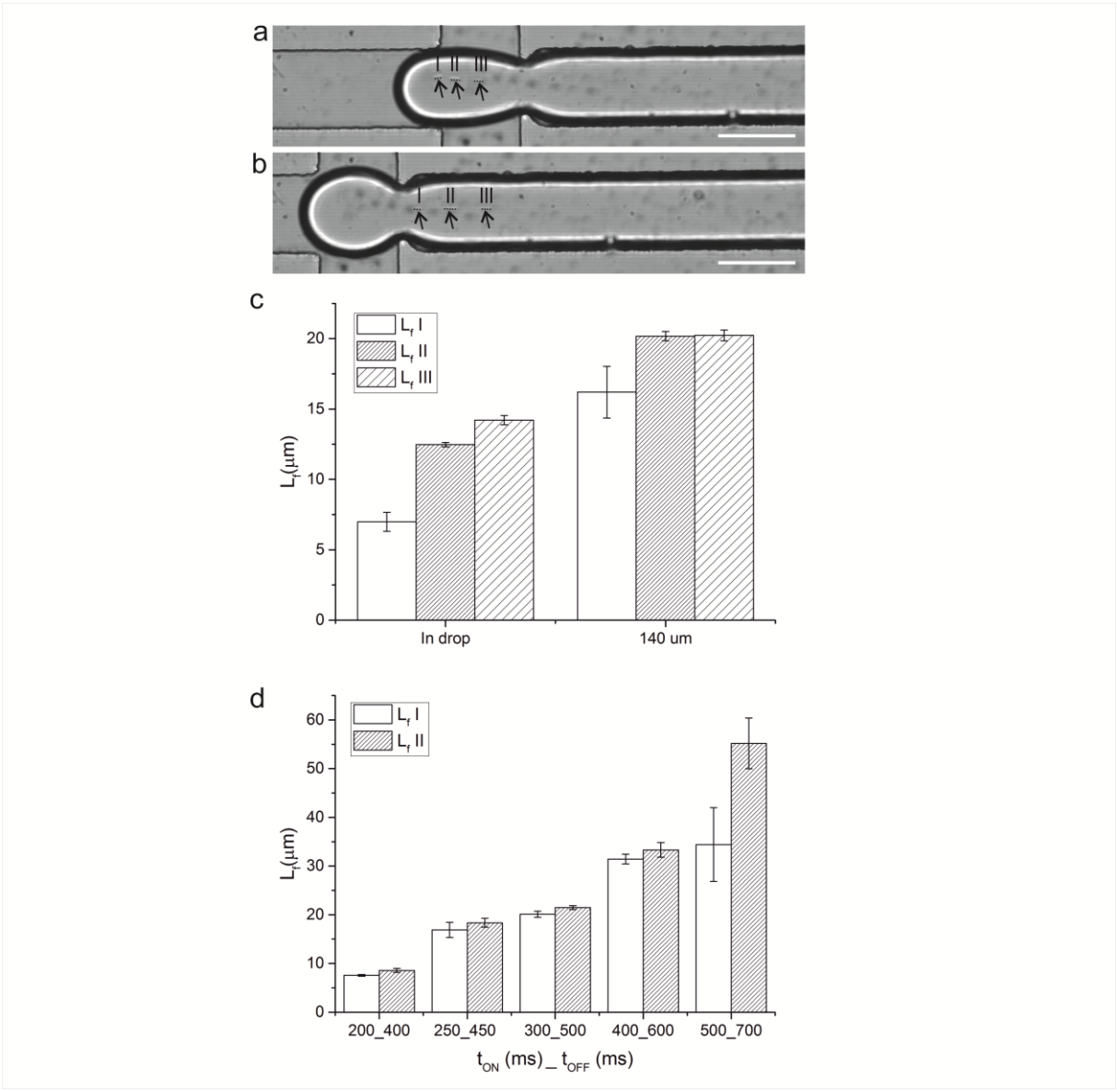

Figure 4. Pulsed UV excitation. UV excitation pulses (200 ms On, 300 ms Off) performed (a) after the cross junction and within forming droplets and (b) at 140 µm before the cross junction, generate in both cases 3 separate fibers. (c) Fiber length comparison at these two positions shows a slight change in fiber length when the excitation is performed before the cross junction. The droplet generation frequencies are 0.52 s^{-1} and 0.49 s^{-1}, for UV excitations either within the droplets or 140 µm before the cross junction, respectively. These values do not significantly differ from those obtained during constant excitation at 145 µm (0.5 s^{-1}). (d) Effects of different pulsed excitation conditions on the fiber's length at 215 µm before the cross junction. At this distance two fibers are generated whose length changes with the increase of the excitation period. In each excitation condition the droplet generation frequencies are: 0.59 s^{-1}, 0.55 s^{-1}, 0.56 s^{-1}, 0.60 s^{-1} and 0.56 s^{-1}. These values do not significantly differ from those obtained during constant UV excitation at 215 µm (0.6 s^{-1}). Scale bar equal to 100 µm.

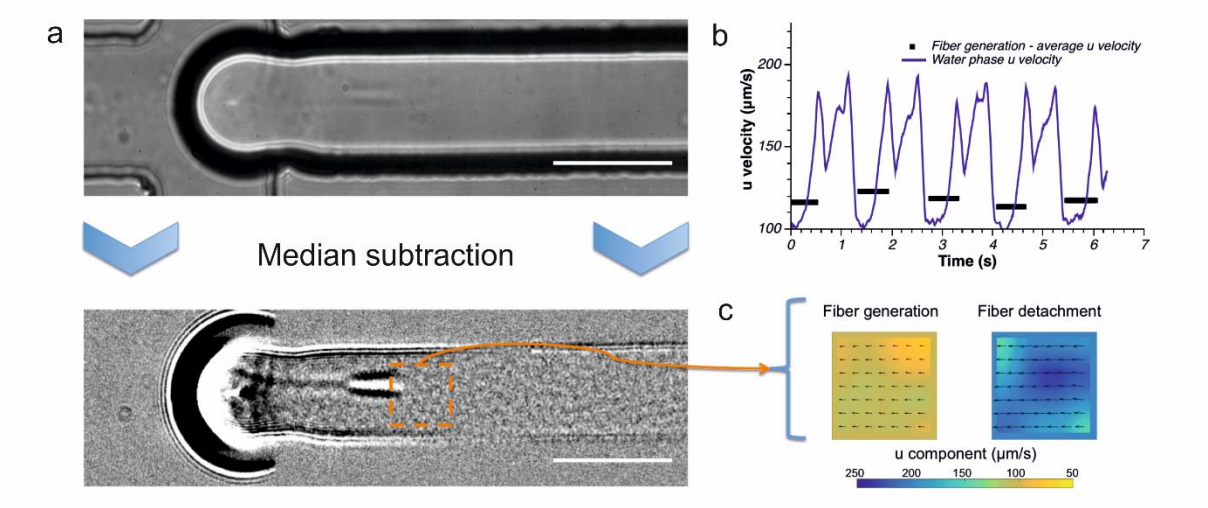

Figure 5. Ghost Particle Velocimetry (GPV) analysis. (a) By seeding the dispersed phase with light-scattering 0.2 µm polystyrene particles it is possible to obtain a speckle pattern by simply subtracting the median obtained from several subsequent images. (b-c) The speckle pattern can be analysed to obtained information on the velocity field where the horizontal velocity (u) of a 55x55 μm^2 region of the dispersed phase was monitored over several droplet generation while, at the same time, PEGDA fibers were produced. When the velocity of the flow falls below 120 µm/s photo-polymerization is initiated and stops when the velocity increases. All data presented refer to a situation where the pressures of the dispersed and continuum phases were, respectively, 40 and 22 mbar, and d_{je}=123 µm. Images were acquired at 200 frames per second with an exposure time of 500 ms. Scale bars are equal to 100 µm.

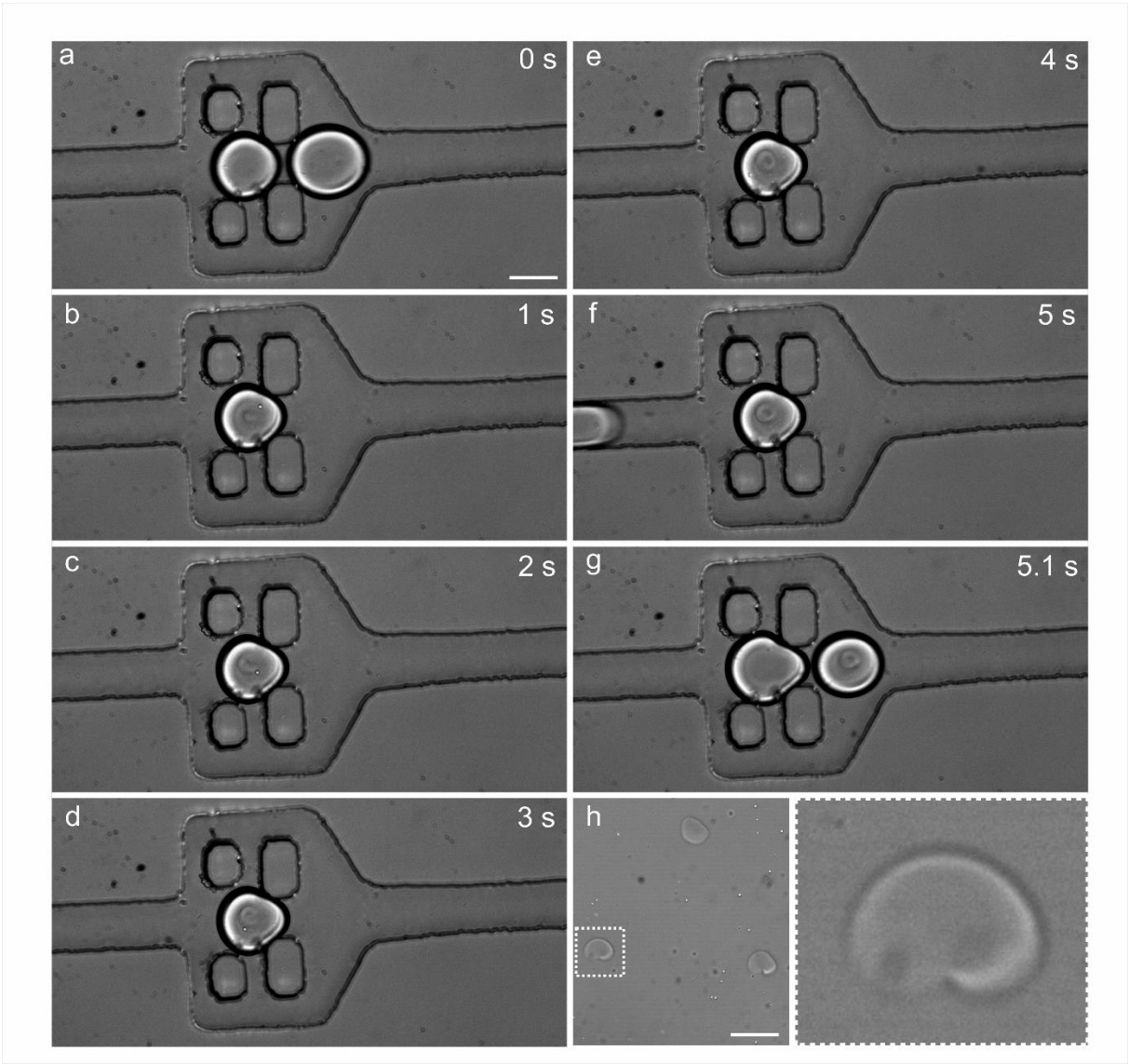

Figure 6. Constant UV excitation in on-line trapped droplets. (a-g) Time sequence of constant UV excitation during droplet trapping. Both the oil and the PEGDA precursor solution are pressurized at 16 mbar, the droplet of PEGDA is generated and trapped by pillars forming a trap. While trapped, the fluid inside the droplet keeps recirculating by the shearing effect of the oil phase that flows around it. (h) Bean-like microgels extracted once the emulsion is broken off. Scale bars are equal to 50 µm.

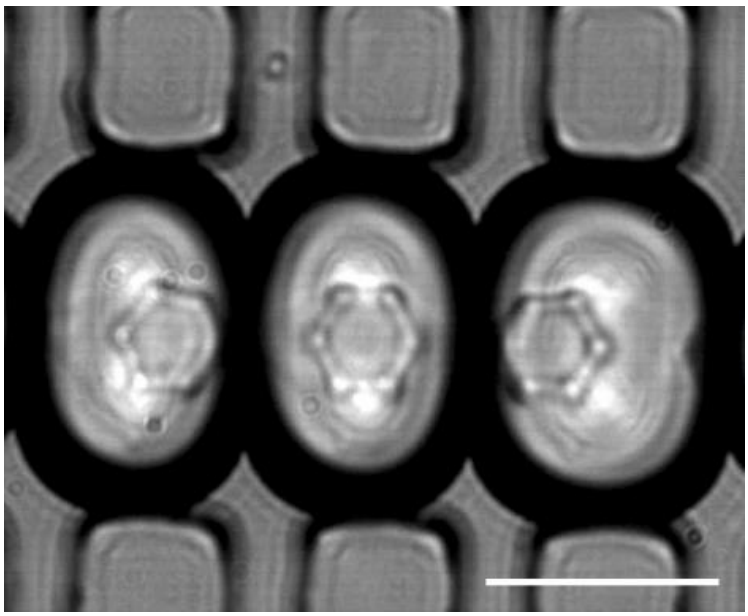

Figure 7. Pulsed UV excitation in trapped droplets under static conditions. Trains of pL volume droplets of PEGDA precursor solution (containing 4% v/v of curing agent) are trapped within a microfluidic device and exposed to a 600 ms UV light pulse after the flow is stopped. The pattern used in the excitation is made of a row of dumbbell hexagon geometries, as shown in Figure 1e. The scale bar is equal to 50 μm.